JBM J Bone Metab 2022;29(4):271-277
https://doi.org/10.11005/jbm.2022.29.4.271
pISSN 2287-6375 eISSN 2287-7029

Case Report

Five-Year Assessment of Multiple Gene Variants Associated with Bone Marrow Hypocellularity, Reduced Bone Density, and Ovarian Insufficiency in Adolescence

E. Scott Sills[1,2], Conor Harrity[3], Samuel H. Wood[2,4]

[1]*Plasma Research Section, FertiGen Center for Advanced Genetics/Regenerative Biology Group, San Clemente, CA;*
[2]*Department of Obstetrics and Gynecology, Palomar Medical Center, Escondido, CA, USA*
[3]*Department of Obstetrics and Gynecology, Beaumont Hospital, Royal College of Surgeons in Ireland, Dublin, Ireland*
[4]*Gen 5 Fertility Center, San Diego, CA, USA*

Corresponding author
E. Scott Sills
Plasma Research Section, FertiGen Center for Advanced Genetics/Regenerative Biology Group, P.O. Box 73910, San Clemente, CA 92673, USA
Tel: +1-949-899-5686
Fax: +1-949-899-5686
E-mail: ess@prp.md

Received: August 20, 2022
Revised: October 12, 2022
Accepted: October 18, 2022

This study covers the 5-year interval prior to COVID-19 admission for an otherwise healthy 46,XX adolescent expanding the developmental characterization of an unusual convergence of amenorrhea and genetic mutations. The patient experienced rapid collapse of endogenous estradiol output followed by secondary amenorrhea at 13 years of age. Euploid, diffusely hypocellular bone marrow was present on biopsy, although anemia or reduced total immunoglobulin production was not identified. Bone density was 1.5 years below mean; multiple dental anomalies were also documented. While alterations in "master regulator" genes *RUNX2, SALL1,* and *SAMD9* are usually diagnosed in early childhood when missed milestones, dysmorphic features, or chronic infection/immune impairment warrant cross-disciplinary evaluation, this study is the first known report to associate ovarian failure with adolescence with such variants. Immunoglobulin patterns, osseous histomorphology, dentition, hematology/renal screening, pelvic anatomy, ovarian reserve data, and thyroid findings are also correlated. Although severe pathology is typically encountered when any of these genes are disrupted alone, this longitudinal survey reveals that a mild phenotype can prevail if these 3 variants occur simultaneously. Periodic monitoring is planned given the unclassified status of this unique mutation set.

Key Words: Genetic variation · Hypocellular marrow · Premature ovarian insufficiency

INTRODUCTION

A 'chief conductor' driving cartilage formation and skeletal development, Runt-related transcription factor 2 (*RUNX2*) is a gene with at least 200 known mutations. Several such variants can manifest as cleidocranial dysplasia, a condition with delayed fontanel closure, enlarged head circumference, clavicular dysmorphia, abnormal dentition, short stature, or hand defects.[1] The frequency of *RUNX2* variants in the general population may be as low as 0.4%.[2] The spalt-like transcription factor 1 (SALL1) gene broadly controls DNA packaging and chromatin remodeling. This gene also coordinates female urogenital structure, and Mullerian de-

Graphical Abstract

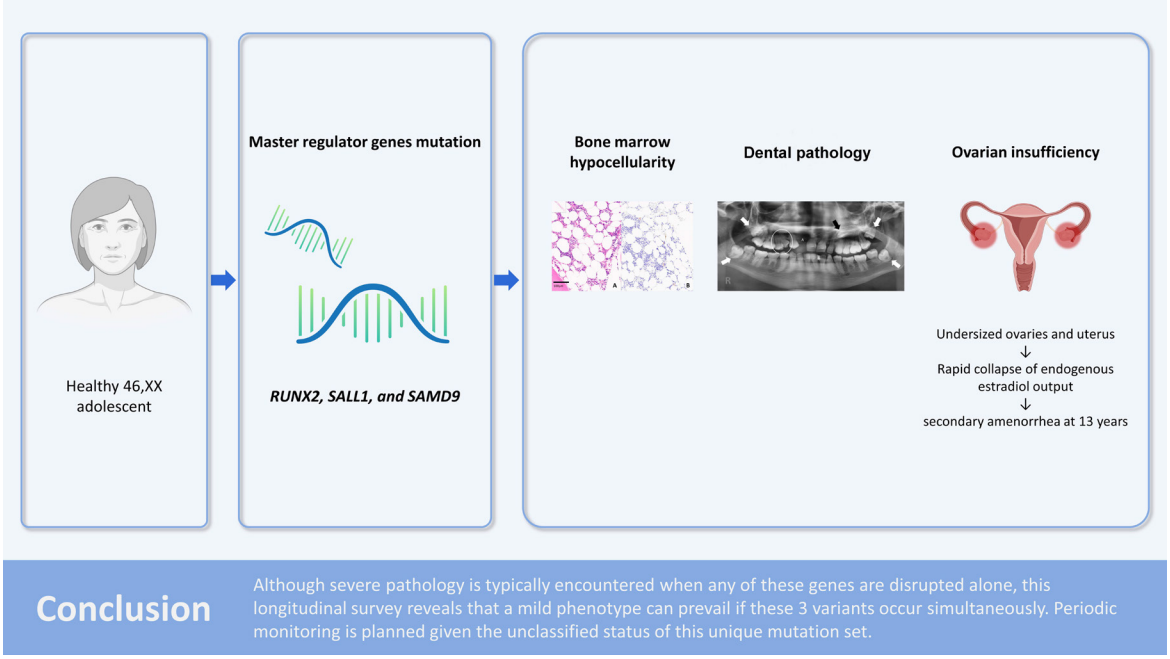

fects can occur with its mutation.[3] *SALL1* also modulates human tumorigenesis with >70 variants now associated with Townes-Brocks syndrome (*i.e.*, otic, limb, renal, and anal anomalies).[4] Such mutations occur with uncertain frequency, but from >3,000 targets with putative association to single gene disorders, *SALL1* was among the least common.[5] The gene for sterile α motif domain-containing protein 9 (*SAMD9*) localizes to a region frequently involved in myeloid malignancies, blood dyscrasias, and childhood immune impairments. That *SAMD9* might be causative in certain hematologic disorders was first advanced by Asou et al. [6] who linked microdeletions at this locus with myeloid malignancies. Germline missense *SAMD9* changes were subsequently implicated in a constellation of features termed MIRAGE syndrome,[7] consisting of myelodysplasia, infection, restricted growth, adrenal hypoplasia, genital anomaly, and enteropathy. Fewer than 50 such cases have been described.[8] The major pathobiological consequences of *RUNX2, SALL1,* or *SAMD9* variants limit the opportunity for longitudinal follow-up, and alteration of all 3 in combination has only been encountered once.[9] The current project was undertaken to enlarge the clinical characterization of this atypical genetic confluence during the adolescent-to-adulthood transition.

CASE REPORT

As the 3 newly discovered variants here were not identified together in any public genome library and the closest partial intersection involving these genes was reported from an animal model,[10] *a priori* pathogenicity estimates could not be calculated. Precautionary bone marrow biopsy was advised to provide tissue for genome-wide single nucleotide polymorphism (SNP) microarray analysis (Illumina Infinium CytoSNP-850Kv1.2 BeadChip; Illumina, San Diego, CA, USA). With disease-associated gene-centric content of >800 K SNP loci from chromosomes 1-22, >29 K and >2 K loci from X and Y chromosomes, respectively, this platform offered a resolution of ~1 probe every 4 kb with an extra 110,000 probes interrogating at least 4 pathology-associated genes, as per ABMG consortium opinion. Nucleotide positions were mapped using the February 2009 assembly of the human reference sequence.[11] The proband's half-sibling also underwent bi-directional sequence analysis for the newly discovered variants in *RUNX2, SALL1,* and *SAMD9* but was negative for all 3 (Table 1). Total

https://doi.org/10.11005/jbm.2022.29.4.271

Table 1. Findings noted in 46,XX non-syndromic *SAMD9*, but absent in half-sibling (46,XY) with common mother

	Location	Coding DNA	Protein product	Coordinates	Variation effect[a]	Parental data
RUNX2[b]	6p21.1	[*duplication*]				mat.dup.
SALL1	16q12.1	759 A>T	Gln253His Q253H	16:51175374	-4.08	mat.var.
SAMD9	7p21.2	2471 G>A	Arg824Gln R824Q	7:92732940	-0.5	*de novo*

Variants reported are inherited as heterozygous/autosomal dominant.
[a]Calculated protein variation effect analysis (Protein Variation Effect Analyzer [PROVEAN]).
[b]3′ duplication corresponds to arr (GRCh37), (45459496_45515207)×3 maternal duplication.
RUNX2, Runt-related transcription factor 2; *SALL1*, spalt-like transcription factor 1; *SAMD9*, sterile α motif domain-containing protein 9.

body bone density was measured on the Lunar Prodigy Advance device (GE Medical Systems, Madison, WI, USA), calibrated at 37 μGy.

Medical information for this intake was gathered after proband's high school graduation to prepare for her relocation to university. Laboratory tests, pathology slides, X-rays, and chart notes for the period corresponding to ages 13 to 18 years were matched with key health events based on patient narrative, contemporary notes, discussion with care team members, and parental interviews. Exome sequence analysis was completed in 2021 during COVID-19 hospitalization and intensive care unit transfer, followed by renal biopsy. Molecular characterization for the patient and both non-consanguineous parents provided an informative pedigree to document variants in *RUNX2*, *SALL1*, and *SAMD9*, as previously described.[9]

Complete blood count (CBC) data were analyzed from routine check-ups between 2016 and 2021, when the patient's most recent body mass index was 17.8 kg/m^2. While this included marginally abnormal indices and occurred with no discernable pattern, the exception was mean corpuscular volume (MCV) which was consistently elevated. The patient had long taken multivitamin supplements for this macrocytosis, and serum folate was normal at 777 ng/mL. Platelet (PLT) concentration was always within the standard range during the review period although mean PLT volume (MPV) was not measured at every visit. When available, MPV was slightly low (data not shown). Flow cytometry immune testing identified nominally elevated CD3$^+$ (ratio) and CD8$^+$ (absolute) cells, an upward shift in the CD4$^+$/CD8$^+$ ratio, and markedly suppressed natural killer cells. Serum immunoglobulin (Ig) A and IgG levels were also marginally reduced, despite normal total Ig and IgM levels (Table 2). Serum blood urea nitrogen (BUN) and creatinine (Cr) levels were unrelated to concurrent CBC fluctuations (Fig. 1A, B).

Whole blood analysis on morning of bone marrow biopsy showed erythrocyte (RBC), hemoglobin, and hematocrit at 3.3×10^6/μL. 11.8 g/dL, and 36.1%, respectively. Leukocyte count (white blood cell) was normal at 5.7 K/μL (reference range, 4.4-9.7). Both MCV and mean corpuscular hemoglobin were elevated at 106.8 fL and 34.9 pg. PLT count was normal at 182 K/μL. Generalized bone marrow hypocellularity was observed with trace storage iron, decreased erythroid precursors with mildly megaloblastoid maturation, decreased granulocyte precursors with full maturation, and normal megakaryocytes (Fig. 2A, B).

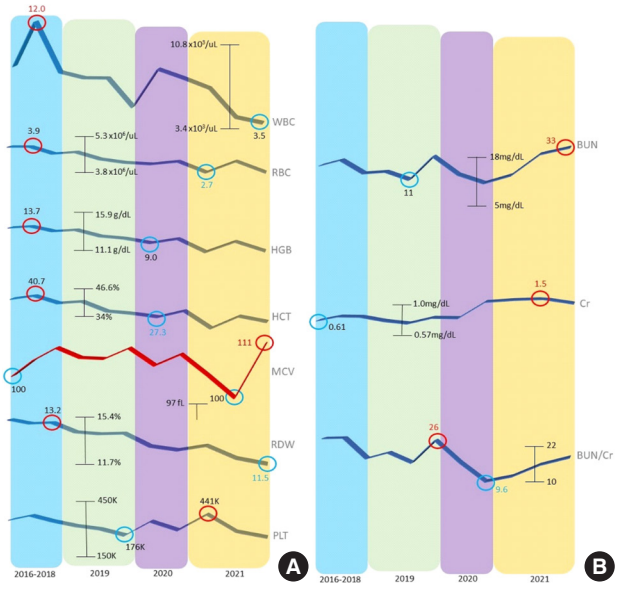

Fig. 1. Trends and high/low screening results for (A) hematopoiesis via complete blood count and (B) renal function via blood urea nitrogen (BUN)/creatinine (Cr), 2016-2021. Note persistently elevated mean corpuscular volume (MCV) (red line). Maximum and minimum values for parameters are circled (abnormal high=red; abnormal low=blue). WBC, white blood cell; RBC, red blood cell; HGB, hemoglobin; HCT, hematocrit; RDW, red cell distribution width; PLT, platelet.

The myeloid:erythroid precursor ratio was normal on core analysis, and no increased fibrosis was evident on reticulin stain. Marrow samples showed high lymphocytes and mono-

Table 2. Summary of complete blood count, differential and immunoglobulin data measured in healthy 46,XX with new variants in *RUNX2, SALL1,* and *SAMD9*

Parameter	Result	Reference range
ABS CD19$^+$ (μL)	153	12-645
%CD19$^+$ (%)	6.1	3.3-25.4
ABS CD3$^+$ (μL)	2,325	622-2402
%CD3$^+$ (%)	93[a]	57.5-86.2
ABS CD4$^+$ helper	868	359-1519
%CD4$^+$ (%)	34.7	30.8-58.5
ABS CD8$^+$ (μL)	1,055[a]	109-897
%CD8$^+$ (%)	42.2[a]	12-35.5
CD4/CD8	0.82[a]	0.92-3.72
ABS NK (CD56/16)	8[b]	24-406
%NK (%)	0.3[b]	1.4-19.4
WBC ($\times 10^3$/μL)	5.5[b]	3.4-10.8
RBC ($\times 10^6$/μL)	3.36[b]	3.77-5.28
HGB (g/dL)	12.1	11.1-15.9
HCT (%)	35.6	34.0-46.6
MCV (fL)	106[a]	79-97
MCH (pg)	36[a]	26.6-33
MCHC (g/dL)	34	31.5-35.7
RDW (%)	11.3[b]	11.7-15.4
PLT ($\times 10^3$/μL)	229	150-450
Neutrophils (%)	47	-[c]
Lymphocytes (%)	45	-[c]
Monocytes (%)	8	-[c]
Eosinophils (%)	0	-[c]
Basophils (%)	0	-[c]
ABS neutrophils ($\times 10^3$/μL)	2.6	1.4-7
ABS lymphocytes ($\times 10^3$/μL)	2.5	0.7-3.1
ABS monocytes ($\times 10^3$/μL)	0.4	0.1-0.9
ABS eosinophils ($\times 10^3$/μL)	0	0-0.4
ABS basophils ($\times 10^3$/μL)	0	0-0.2
Immature gran (%)	0	-[c]
ABS Immature gran ($\times 10^3$/μL)	0	-[c]
Ig - total (g/dL)	2.4	1.5-4.5
IgA (mg/dL)	64[b]	87-352
IgG (mg/dL)	559[b]	719-1475
IgM (mg/dL)	197	58-230

[a]Above normal.
[b]Below normal.
[c]Reference range not specified/undefined.
ABS, absolute; NK, natural killer cell; WBC, white blood cell; RBC, red blood cell; HGB, hemoglobin; HCT, hematocrit; MCV, mean corpuscular volume; MCHC, mean corpuscular hemoglobin concentration; RDW, red cell distribution width; PLT, platelet; Ig, immunoglobulin; IgA, immunoglobulin A; IgG, immunoglobulin G; IgM, immunoglobulin M; *RUNX2*, Runt-related transcription factor 2; *SALL1*, spalt-like transcription factor 1; *SAMD9*, sterile α motif domain-containing protein 9.

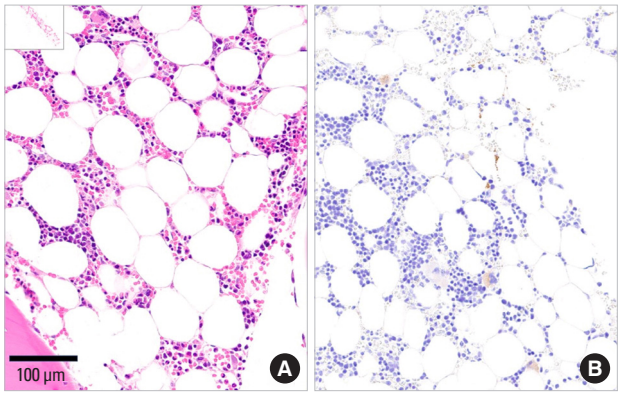

Fig. 2. Marrow hypocellularity with compound heterozygous variants involving *RUNX2, SALL1,* and *SAMD9*, showing predominant adipose cells and reduced hematopoiesis. (A) Hematoxylin and eosin (H&E) stain, (B) CD61 stain (×20 magnification).

cytes (43.5 and 6%, respectively), low bands (5.5%; reference range, 17-33) and nominally elevated orthochromatic normoblasts (7.5%; reference range, 1-5). Fluorescent *in situ* hybridization demonstrated a normal signal with no copy number variance in nuclei (N=200). Bone marrow cytogenetics verified a non-mosaic 46,XX karyotype, aligning with results obtained earlier from peripheral (somatic) samples. The fragile X carrier panel was negative. At age 15 years, her bone age via standard radiograph was below mean, consistent with age 13.5 years. Bone density assessment identified low bone density, with height-adjusted Z-scores of -0.7 and -1.6 for axial (spine) and total (sub-cranial) body, respectively.

By age 7 years, all deciduous teeth were succeeded by permanent teeth, although anomalous non-descent of left cuspid was incidentally identified during pre-orthodontic screening. In addition, a panoramic X-ray at age 17 years revealed multiple underdeveloped roots and secondary loss of right lateral incisor. Surgery to remove all 4 impacted wisdom teeth (Fig. 3) is scheduled.

Menarche was at age 11 years but only one spontaneous menses followed; within 2 years menses had ceased. At age 15.5 years, low-dose oral contraceptives were initiated to restore cyclicity, and no other hormonal therapy was ever prescribed. Serum follicle-stimulating hormone was consistently >100 mIU/mL with anti-Müllerian hormone below measurement threshold (<0.015 ng/mL). Small ovaries were seen on abdominal ultrasound, including sparse but active bilateral follicular response on the clomiphene challenge test, and pre-replacement serum estradiol levels

https://doi.org/10.11005/jbm.2022.29.4.271

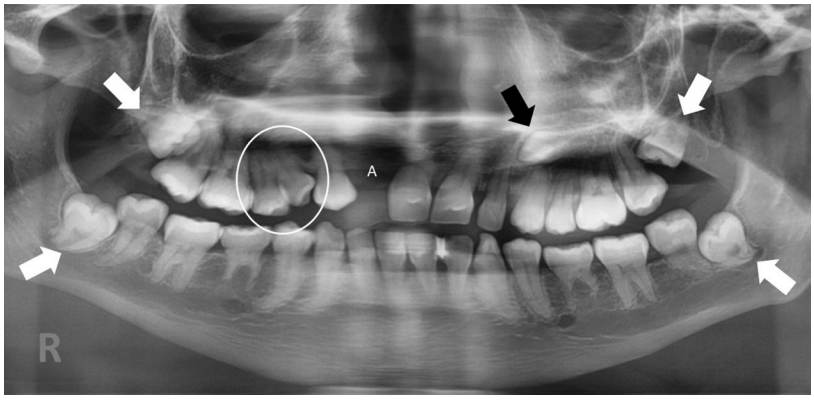

Fig. 3. Panorex view at age 17 years indicating third molar impaction (white arrows), near-horizontal malposition of left maxillary cuspid (black arrow), and contralateral cuspid/bicuspid transposition (circle). Diffuse root hypoplasia likely contributed to loss of right maxillary lateral incisor (A).

were regularly <5 pg/mL, all indicative of diminished ovarian reserve.[12] Anti-ovarian antibody test was negative. At age 16, a solitary 2 cm right anterior neck mass was evaluated; laboratory tests were negative for autoimmune involvement and found no evidence of abnormal thyroid or parathyroid function. The structure was nontender and was palpable only after singing. Fine needle aspiration of the lesion showed Bethesda category III cytology; molecular testing found a missense c.1358T>C mutation in the thyroid-stimulating hormone (TSH) receptor gene with a variant allele frequency of 46%, negative for gene fusions or copy number variants.

DISCUSSION

Transcription factors set the pace and pattern of nuclear DNA conversion to mRNA. From amidst more than 1,500 such factors, *RUNX2, SALL1,* and *SAMD9* are especially prominent. The genes coding for these products thus controls cell division, migration, body plan architecture, and apoptosis. While disruption of these factors typically is poorly tolerated, our patient had an active, healthy childhood while carrying variants in all 3. Remarkably, the most dramatic highlight against a rather ordinary pediatric background was her hospitalization for COVID-19. Attribution of findings discussed here to genetic etiologies vs. COVID-19 is challenging, given the unclear status of the specified variants and the expansive, evolving nature of 'Long COVID'. Curiously, the high MPV seen with COVID-19 infection documented by others [13] was absent here. Perhaps the 3 variants dampened MPV by altering individual PLT responsiveness, even though overall PLT number was unaffected. Likewise, the observed low serum IgA and IgG levels alongside normal total Ig may reflect a synthesis of coordinated action by these variants.

Some 150 mutations in *SAMD9* have been associated with outcomes ranging from spontaneous remission to malignant progression.[14] Most *SAMD9* variants presage early death from myeloid dysplasia, immune system imbalance, adrenal insufficiency, or chronic undernourishment from feeding difficulty.[15] *SAMD9* mutations via germline transmission predispose to low PLTs, acquired monosomy 7, constitutional abnormalities (e.g., ambiguous genitalia) and immune dysfunction.[16] Less is known about *SAMD9* variants which appear as *de novo* events. Computer modeling has envisioned a protein-protein interaction network of differentially expressed genes, and human *SAMD9* was among the 'hub genes' having special relevance after SARS-CoV-2 infection.[17] Thomas et al. [18] assessed the functional impact of wild-type and mutant *SAMD9* in primary mouse or human hematopoietic stem and progenitor cells. Using protein interactome analyses, transcriptional profiling, and functional validation, it was concluded that *SAMD9* mutations tend to favor interference with DNA damage repair and ultimately apoptosis in hematopoietic cells.[18] The hypocellular terrain noted here on bone marrow biopsy may be a partial expression of this *SAMD9* influence.

RUNX2 is considered a centrally regulating transcription factor for osteoblast and chondrocyte differentiation and overall skeletal architecture.[19,20] Some 80 variants in *RUNX2* have been identified [1] and while heterozygous loss of function mutations can lead to cleidocranial dysplasia, this is inconsistent. Triplication or quadruplication of *RUNX2* accompanies more serious syndromic phenotypes, including coronal/sagittal synostosis or pan-craniosynostosis, suggesting a dosage effect. For our patient, sequence

analysis did identify a 3′ duplication involving at least exons 6 through 9 of *RUNX2*,[9] as plausible contributors both to microscopic (hypocellular) and macroscopic (reduced density) osseous features observed here.

In late adolescence or early adulthood third molar impaction is not unusual, and others have investigated differential expression of *RUNX2* regarding tooth location before surgical removal. While *RUNX2* was not implicated, another transcription factor (muscle segment homeobox 1 [MSX1]) was differentially expressed depending on the depth of molar impaction, and RUNX2 is partially controlled by MSX1. As alveolar bone remodeling is central to orthodontic tooth movement, a novel regulatory mechanism whereby FOXO3 induces osteocalcin transcription by promoter activation in concert with *RUNX2* could help explain dental features in this case.

The T>C mutation in codon 453 of the TSH receptor (TSHR) gene found here was previously reported in the setting of nonautoimmune hyperthyroidism—but without *RUNX2*, *SALL1*, or *SAMD9* involvement. Wide tissue expression of TSHRs is well established and includes brain, bone marrow, lymphocytes, pituitary, thymus, testes, kidney, adipose tissue, and fibroblasts. While oocyte growth is influenced via TSHR/cyclic adenosine monophosphate signaling, there has been no reason to obtain ovarian tissue sampling in this patient. A pelvic ultrasound will be useful to identify any changes in gross ovarian anatomy. Similarly, tracking thyroid size, nodularity, and tenderness, as well as the thyroid laboratory panel will be important.

Concerning *SALL1*, some 50 different mutations are currently known. *SALL1* and *RUNX2* may have special relevance in human reproduction. Mammalian estrogen receptor (ER)-β is required for ovarian follicles to advance past the antral stage, and work in rat granulosa cells has placed *RUNX2* within the ER-β-regulated genes directing folliculogenesis, oocyte maturation and ovulation. While *SALL1* is essential for stem cell maintenance in kidney, heart, and spermatogonial progenitors,[4] its role in human ovarian tissue awaits better characterization.

The Venn diagram for worldwide clinical experience with *RUNX2, SALL1*, and *SAMD9* returned a null union set prior to this patient. The detrimental consequences of mutation of these genes in isolation may have been mitigated by the chance occurrence of all 3 variants in concert—an offset possibly enabled by cross-gene effects or epigenetic silencing.[9] Monitoring for patients with a *SAMD9* variant includes CBC with differential every 6 months, and repeat bone marrow aspirate/biopsy (and karyotype) should anemia, thrombocytopenia, or neutropenia develop.[8] Red blood cell dysplasia, agglutination, or fragmentation are unlikely given the low/normal red-cell distribution width measured here. Serum BUN and Cr levels evidenced no discernable pattern whenever these were abnormal but as cystatin-C may be superior to BUN/Cr to detect early-stage disease, a screening panel including all 3 will guide the need for repeat renal biopsy. To guard against further loss in bone mineral content, the current oral contraceptive pills regime will be maintained with annual DXA. As this case incorporates a *de novo* variant, the risk to siblings is considered somewhat greater than the background population [8] and cytogenetic testing for an older half-brother was reassuring. Clinical guidelines for these variants have not been developed due to their exceptionally low frequency, and this underscores an important limitation of our report—it is impossible to assign specific genetic causality to such rare events. Because not all instances of marrow hypocellularity will render immediate effects, periodic reassessment is essential.

DECLARATIONS

Authors' contributions

Conceptualization: ESS, CH, and SHW; Data curation: ESS, CH, and SHW; Methodology: CH, and SHW; Writing - original draft: ESS; Writing - review & editing: ESS, CH, and SHW; All authors read and approved the final manuscript.

Ethics approval and consent to participate

Not applicable; written permission was provided by the patient and family for publication of this manuscript.

Conflict of interest

No potential conflict of interest relevant to this article was reported.

ORCID

E. Scott Sills *https://orcid.org/0000-0001-7334-1031*
Conor Harrity *https://orcid.org/0000-0001-6528-9704*

https://doi.org/10.11005/jbm.2022.29.4.271

REFERENCES

1. Hansen L, Riis AK, Silahtaroglu A, et al. RUNX2 analysis of Danish cleidocranial dysplasia families. Clin Genet 2011; 79:254-63. https://doi.org/10.1111/j.1399-0004.2010.01458.x.
2. Morrison NA, Stephens AA, Osato M, et al. Glutamine repeat variants in human RUNX2 associated with decreased femoral neck BMD, broadband ultrasound attenuation and target gene transactivation. PLoS One 2012;7:e42617. https://doi.org/10.1371/journal.pone.0042617.
3. Tian W, Chen N, Ye Y, et al. A genotype-first analysis in a cohort of Mullerian anomaly. J Hum Genet 2022;67:347-52. https://doi.org/10.1038/s10038-021-00996-w.
4. Álvarez C, Quiroz A, Benítez-Riquelme D, et al. SALL proteins; Common and antagonistic roles in cancer. Cancers (Basel) 2021;13:6292. https://doi.org/10.3390/cancers-13246292.
5. López-Rivera JA, Pérez-Palma E, Symonds J, et al. A catalogue of new incidence estimates of monogenic neurodevelopmental disorders caused by de novo variants. Brain 2020;143:1099-105. https://doi.org/10.1093/brain/awaa051.
6. Asou H, Matsui H, Ozaki Y, et al. Identification of a common microdeletion cluster in 7q21.3 subband among patients with myeloid leukemia and myelodysplastic syndrome. Biochem Biophys Res Commun 2009;383:245-51. https://doi.org/10.1016/j.bbrc.2009.04.004.
7. Narumi S, Amano N, Ishii T, et al. SAMD9 mutations cause a novel multisystem disorder, MIRAGE syndrome, and are associated with loss of chromosome 7. Nat Genet 2016;48: 792-7. https://doi.org/10.1038/ng.3569.
8. Tanase-Nakao K, Olson TS, Narumi S. MIRAGE syndrome. In: Adam MP, Everman DB, Mirzaa GM, et al., editors. GeneReviews®. Seattle, WA: University of Washington, Seattle; 1993-2022.
9. Sills ES, Wood SH. Phenotype from SAMD9 mutation at 7p21.2 appears attenuated by novel compound heterozygous variants at RUNX2 and SALL1. Glob Med Genet 2022; 9:124-8. https://doi.org/10.1055/s-0041-1740018.
10. Lin Y, Xiao Y, Lin C, et al. SALL1 regulates commitment of odontoblast lineages by interacting with RUNX2 to remodel open chromatin regions. Stem Cells 2021;39:196-209. https://doi.org/10.1002/stem.3298.
11. Axelrod N, Lin Y, Ng PC, et al. The HuRef browser: a web resource for individual human genomics. Nucleic Acids Res 2009;37:D1018-24. https://doi.org/10.1093/nar/gkn-939.
12. Sills ES, Alper MM, Walsh AP. Ovarian reserve screening in infertility: practical applications and theoretical directions for research. Eur J Obstet Gynecol Reprod Biol 2009;146: 30-6. https://doi.org/10.1016/j.ejogrb.2009.05.008.
13. Comer SP, Cullivan S, Szklanna PB, et al. COVID-19 induces a hyperactive phenotype in circulating platelets. PLoS Biol 2021;19:e3001109. https://doi.org/10.1371/journal.pbio.3001109.
14. Sahoo SS, Kozyra EJ, Wlodarski MW. Germline predisposition in myeloid neoplasms: Unique genetic and clinical features of GATA2 deficiency and SAMD9/SAMD9L syndromes. Best Pract Res Clin Haematol 2020;33:101197. https://doi.org/10.1016/j.beha.2020.101197.
15. Rentas S, Pillai V, Wertheim GB, et al. Evolution of histomorphologic, cytogenetic, and genetic abnormalities in an untreated patient with MIRAGE syndrome. Cancer Genet 2020;245:42-8. https://doi.org/10.1016/j.cancergen.2020.06.002.
16. Sahoo SS, Pastor VB, Goodings C, et al. Clinical evolution, genetic landscape and trajectories of clonal hematopoiesis in SAMD9/SAMD9L syndromes. Nat Med 2021;27:1806-17. https://doi.org/10.1038/s41591-021-01511-6.
17. Xie TA, He ZJ, Liang C, et al. An integrative bioinformatics analysis for identifying hub genes associated with infection of lung samples in patients infected with SARS-CoV-2. Eur J Med Res 2021;26:146. https://doi.org/10.1186/s40001-021-00609-4.
18. Thomas ME, 3rd, Abdelhamed S, Hiltenbrand R, et al. Pediatric MDS and bone marrow failure-associated germline mutations in SAMD9 and SAMD9L impair multiple pathways in primary hematopoietic cells. Leukemia 2021;35: 3232-44. https://doi.org/10.1038/s41375-021-01212-6.
19. Otto F, Thornell AP, Crompton T, et al. Cbfa1, a candidate gene for cleidocranial dysplasia syndrome, is essential for osteoblast differentiation and bone development. Cell 1997; 89:765-71. https://doi.org/10.1016/s0092-8674(00)80259-7.
20. Matthijssens F, Sharma ND, Nysus M, et al. RUNX2 regulates leukemic cell metabolism and chemotaxis in high-risk T cell acute lymphoblastic leukemia. J Clin Invest 2021;131: e141566. https://doi.org/10.1172/jci141566.